

Field-free alignment in repetitively kicked nitrogen gasJames P. Cryan,^{1,2} Philip H. Bucksbaum,^{1,2,3} and Ryan N. Coffee^{1,4}¹*The PULSE Institute for Ultrafast Energy Science, SLAC National Accelerator Laboratory, 2575 Sand Hill Road, Menlo Park, California 94025, USA*²*Department of Physics, Stanford University, Stanford, California 94305, USA*³*Department of Applied Physics, Stanford University, Stanford, California 94305, USA*⁴*The Linac Coherent Light Source, SLAC National Accelerator Laboratory, 2575 Sand Hill Road, Menlo Park, California 94025, USA*

(Received 15 May 2009; published 7 December 2009)

We demonstrate a high level of laser-induced transient alignment in room temperature and density N_2 with a technique that avoids laser field ionization. Our measured alignment shows an improvement over previous one-pulse or two-pulse experimental alignment results and approaches the theoretical maximum value. We employ eight equally spaced ultrafast laser pulses with a separation that takes advantage of the periodic revivals for the ensemble of quantum rotors. Each successive pulse increases the transient alignment $[\langle \cos^2 \theta \rangle(t)]$ and also moves the rotational population away from thermal equilibrium. These measurements are combined with simulations to determine the value of $\langle \cos^2 \theta \rangle$, the J -state distributions, and the functional dependencies of the alignment features.

DOI: [10.1103/PhysRevA.80.063412](https://doi.org/10.1103/PhysRevA.80.063412)

PACS number(s): 33.80.-b, 42.50.Hz

Highly aligned molecules in gas phase are important for angle resolved studies where the degree of alignment is directly related to the structural resolution. High-order harmonic generation (HHG) and nonsequential double ionization (NSDI) both show a dependence on the angle between the molecular axis and the probe polarization. Increased angular resolution in these studies facilitates a better comparison between experiment and theory. X-ray experiments designed to measure differential cross sections or to produce tomographiclike structural images also depend on independent determination of the molecular alignment. X-ray processes typically involve small total cross-sections and therefore such experiments would require relatively high target densities. Alignment of molecular gas at STP or greater not only will enhance HHG studies in room-temperature environments like capillary waveguides but also it will enable gas-phase x-ray studies in the ultrafast regime.

Techniques for laser alignment of molecular gases can be divided into two regimes, adiabatic, or impulsive, depending on the relative duration of the laser pulse and the average time of rotation of the molecules in the ensemble [1]. Adiabatic laser-induced molecular alignment occurs at the peak of a strong aligning laser field; this limits the generality of the method. Impulsive Raman excitation creates nonstationary rotational wave packets that exhibit field-free transient alignment. Supersonic coexpansion with a dense ideal gas is commonly used to lower the rotational temperature in order to improve the transient alignment [2,3]. However, the presence of the dense buffer gas complicates studies in HHG, NSDI, and precludes most x-ray experiments.

Many theoretical papers have proposed using quantum control methods to optimize the field-free alignment of molecules. Quantum control methods can be used to shape the excitation pulse to optimize the aligned state [4–7]. Other control schemes exploit the timing and intensity ratio of multiple pulses to achieve optimal alignment [8–12]. Previous experimental studies have demonstrated the benefit of two pulses [13–16], but in this paper, we report our implementation of a train of eight identical laser pulses separated by the

rotational revival as an alignment technique for room temperature thermal ensembles.

Most previous efforts (both theoretical and experimental) using multiple pulses apply additional pulses at the revival of the maximum alignment signal. This technique has been shown to increase the alignment in both cold and warm gases [9,10,12,14,16]. Our multiple pulse technique uses a train of equal-energy pulses acting at the “quantum echoes” of the initial pulse, i.e., when the density matrix, $\rho(t)$, returns to the value it has immediately after the previous impulse. At the quantum echo the ensemble is once again isotropic, and this is the time when we apply the next laser pulse, not at the peak of the transient alignment which occurs slightly later [13]. Pumping at quantum echoes produces a high field-free transient alignment, which can be quantified by the expectation value of the $\cos^2 \theta$ operator, $\langle \cos^2 \theta \rangle(t) = \text{tr}[\rho(t)\cos^2 \theta]$. This pumping scheme also exhibits a large time-averaged alignment $\langle \langle \cos^2 \theta \rangle \rangle_t$, where $\langle \rangle_t$ denotes a time average over one revival period.

$$\langle \langle \cos^2 \theta \rangle \rangle_t = \text{tr}[\text{diag}(\rho)\cos^2 \theta] = \sum_{J,M} \rho_{JMJM} \langle J,M | \cos^2 \theta | J,M \rangle. \quad (1)$$

The time-averaged alignment is often referred to as the population alignment [4]. A high value is indicative of strong Raman redistribution among the available m_J -conserving angular momentum states.

In this paper, we report a high degree of alignment in nitrogen at STP resulting from impulsive-Raman excitation with a train of eight linearly polarized laser pulses. Our multiple impulse technique exploits the revival structure of $\rho(t)$ with pulses separated by the revival period of the density matrix, $\tau_{\text{rev}} = \frac{1}{2B}$ [8,13]. First, we describe the experimental apparatus that we use to create and analyze the molecular alignment. Then we discuss the mechanics of our time-dependent density matrix calculation which we use to calibrate the alignment signal. Next, we show that the eight-

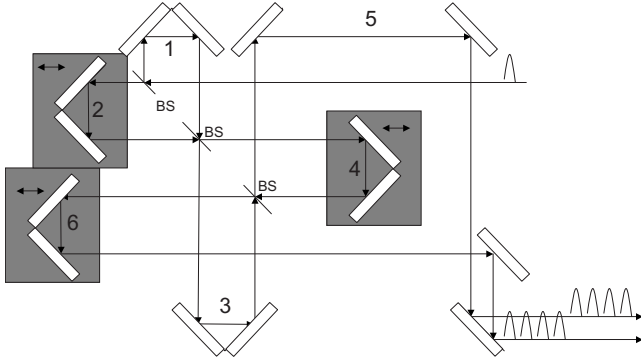


FIG. 1. Nested interferometer design to produce eight equally spaced pulses [17]. The optical path difference between arms 1 and 2 is ~ 8.4 ps, 3 and 4 is ~ 16.8 ps, and 5 and 6 is ~ 33.6 ps such that the spacing between pulses is ~ 8.4 ps. This is the rotational period $\frac{1}{2B}$, where B is the rotational constant for molecular nitrogen.

pulse technique achieves alignment that approaches the single impulse physical limit for a room temperature ensemble. Finally, we discuss how the J -state distribution, and likewise the energy of the ensemble, move markedly away from a thermal distribution while the entropy and quantum purity remain unchanged.

We use ~ 50 fs 800 nm pulses at 1 kHz. Three nested interferometers [17], shown in Fig. 1 produce eight equal-energy pulses with interpulse delays that correspond to the full rotational revival for the thermal ensemble, $\tau_{\text{rev}} = 8.35$ ps for N_2 at 300 K [18]. The pulses are set to coincide with the “echo” of the initial pulse. The two displaced but parallel output arms are focused to produce overlapping but crossed focal volumes that do not suffer relative pulse-front tilt. An iris near the final focusing optic sets the pump beam waist.

We measure the optical birefringence of the medium with a ~ 50 fs, 400 nm, circularly polarized probe pulse to quantify the degree of alignment [19–21]. We combine this probe beam with the eight-pulse train using a normal-incidence (T800/R400) dichroic mirror. Probe and pump beams propagate parallel to each other such that a $f \approx 100$ mm off-axis parabola produces overlapping focal volumes that cross at a small angle ($\leq 6^\circ$) inside a windowless nitrogen cell. Prior to the interaction volume, the electric field of the probe beam is given by

$$\vec{F}_1(\vec{x}, t) = \Re \left\{ \frac{|F_0|}{\sqrt{2}} (\hat{x} + e^{i\Delta} \hat{y}) e^{i(kz - \omega t)} \right\}. \quad (2)$$

The pulse propagates along the z axis with wave number k and angular frequency ω . $|F_0|$ is the magnitude of the electric field, \hat{x} is the horizontal direction, and \hat{y} is the vertical. We choose the phase difference between the different polarizations to be $\Delta = \frac{\pi}{2}$ for circular polarization. The aligning pump pulses are horizontally polarized (x axis) such that the aligned gas produces a transient “slow” axis along x . As the circular probe passes through the aligned sample, its \hat{x} polarization gains a phase shift of δ relative to its \hat{y} polarization component such that the electric field of the probe following the interaction volume is given by

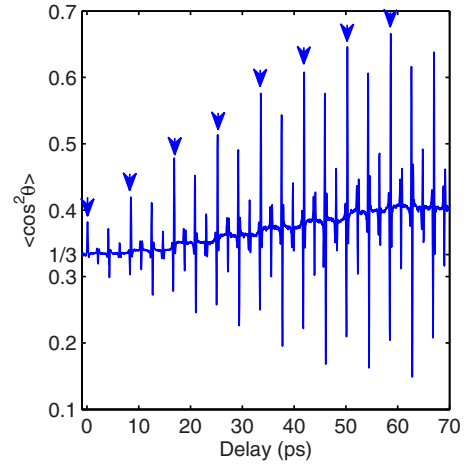


FIG. 2. (Color online) Alignment signal, $\langle \cos^2 \theta \rangle$, as a function of probe pulse delay for an eight-pulse train produced by the interferometer setup of Fig. 1. The value of $\langle \cos^2 \theta \rangle$ is calibrated by comparing to simulation which also determines the single-pulse irradiance to be 3.6×10^{13} W/cm 2 . The probe pulse will experience an optical Kerr effect during initial alignment and the first seven revivals (blue arrows) when it overlaps with the pump pulse. We estimate the contribution from the Kerr effect to be $\sim 10\%$ of the signal by comparing the 7th and 8th full revival peaks. This estimate is confirmed by observing the difference between the full and half revivals because the half revivals are entirely field free.

$$\vec{F}_2(\vec{x}, t) = \Re \left\{ \frac{|F_0|}{\sqrt{2}} (\hat{x} + e^{i(\Delta - \delta)} \hat{y}) e^{i(kz - \omega t)} \right\} \quad (3)$$

We separate the probe pulse from the aligning pump pulses with a 45° (T800/R400) dichroic mirror after which we analyze the probe using a $\hat{p} = \frac{1}{\sqrt{2}}(\hat{x} - \hat{y})$ transmission polarizer. The signal recorded by a fast photodiode is proportional to the intensity of the transmitted light or

$$\langle (\vec{F}_2 \cdot \hat{p})^2 \rangle_t = \frac{|F_0|^2}{4} [1 - \cos(\Delta - \delta)]|_{\Delta = \pi/2} = \frac{|F_0|^2}{4} (1 - \sin \delta) \quad (4)$$

Equation (4) shows that a circular probe polarization can be analyzed to give a signal that varies in direct proportion to the alignment-induced phase shift, for small shifts of course. The signal given by Eq. (4) has a large offset, $\frac{|F_0|^2}{4}$, which can be removed by background subtraction. An optical chopper is placed in the pump arm before the beams are recombined. The background signal is removed by subtracting the pump-free birefringence measurement from the measurement when the pump beam is present. A typical signal, with the background subtracted, is shown as a function of optical delay in Fig. 2. To further reduce the noise, a small portion of the probe beam is monitored with another fast photodiode and this signal is used to normalized each laser shot.

We compare our data with quantum simulations to calibrate the experimental value of $\langle \cos^2 \theta \rangle$. Our simulations propagate the full rotational density matrix according to

$$i\hbar \frac{\partial \rho}{\partial t} = [H_{\text{eff}}(t), \rho], \quad (5)$$

were ρ is the density matrix and $H_{\text{eff}}(t)$ is the effective Hamiltonian in the interaction picture, neglecting decoherence. We find the effective Hamiltonian for the ground vibronic state,

$$H_{\text{eff}}(t) = E_J - \frac{1}{4} F^2(t) \Delta\alpha \cos^2 \theta, \quad (6)$$

where $F(t)$ is the electric field envelope, $\Delta\alpha$ is the difference between the parallel and perpendicular static polarizabilities, and θ is the angle between the molecular axis and the polarization of the laser field [22]. The energy of the free rotor is given by, $E_J = BJ^2 - DJ^4$, where J is the angular momentum operator, B is the rotational constant, and D is the centrifugal distortion constant. The solution to the propagation equation is given by

$$\rho(t) = U(t, t_0) \rho(t_0) U(t, t_0)^\dagger, \quad (7)$$

$$U(t, t_0) = \exp\left(\frac{-i}{\hbar} \int_{t_0}^t H_{\text{eff}}(t') dt'\right). \quad (8)$$

We use a split operator method to calculate the propagator for time steps of 1 fs over a 50 fs full width at half-maximum cosine squared pulse envelope. It is common to approximate a Gaussian temporal shape with a cosine squared envelope to preserve the time-bandwidth product while suppressing artificial, numerically induced population transfer from the hard turn-on or turn-off of a truncated Gaussian. Calculations using a true impulse (i.e., a zero width pulse) achieved similar results but the 50 fs pulse better approximates our experimental conditions. We use a 10 fs step to track the free rotation between the pulses. These pulses are spaced by an optimal separation of 8.37 ps which is consistent with the full revival period for the thermal ensemble.

Our calculations show that the maximum transient alignment grows linearly for low pulse irradiance while the population alignment grows quadratically with pulse irradiance. We use a least-squares fit to the ratio of peak alignment to population alignment to obtain the average focal irradiance and scale the data to obtain the calibration for $\langle \cos^2 \theta \rangle$. We measure a decoherence time of roughly $1/\gamma \sim 80$ ps and so we fit only the first three revivals (~ 25 ps) to minimize the effect caused by decoherence. In Fig. 3 the simulation and data are plotted in the vicinity of the first (left) and eighth (right) revivals. We see from the left and right panels of Fig. 3(a) that both early (left) and late (right) revival features match the simulation quite well. For the subsequent panels, we see that the population alignment signal from experiment and simulation also agree quite well. Any degradation of such agreement for the coherent signal is due to the combined effects: focal volume averaging, probe-duration convolution, and collisional decoherence. Furthermore, for the highest laser intensity we begin to see over-rotation of the signal, i.e., the signal begins to deviate from the expected linear dependence on alignment, described in and after Eq. (4).

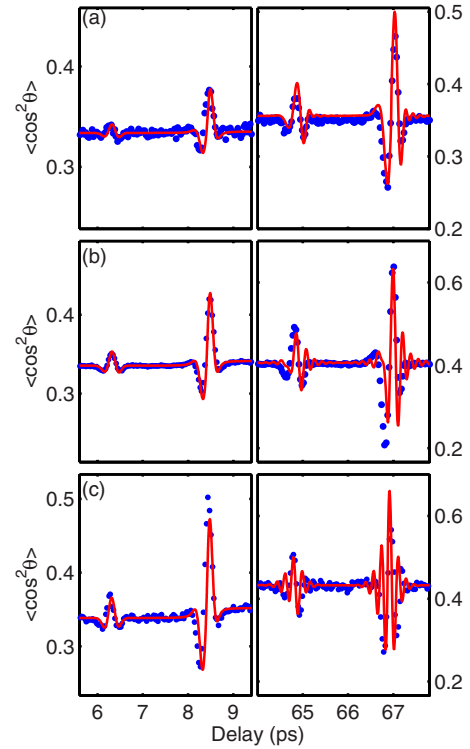


FIG. 3. (Color online) Simulation (line) and experimental data (dots) for the first three-quarter and full revivals (left) and the eighth three-quarter and full revivals (right) for (a) 1.7×10^{13} W/cm², (b) 3.6×10^{13} W/cm², (c) 5.4×10^{13} W/cm².

For our eight-pulse technique, the single-pulse intensity dependence is actually encoded in the stair-step pattern of Fig. 2. It can be easily shown that Raman transitions induce coherences that grow linearly with single-pulse irradiance while Raman population transfer grows quadratically. These two functional dependencies are directly reflected in a time-streaked fashion in Fig. 2. A large population alignment reflects a nonthermal J -state distribution and Fig. 4 shows the calculated J -state distribution as a function of pulse number. We see in Fig. 4(d) that the final J -state distribution is decid-

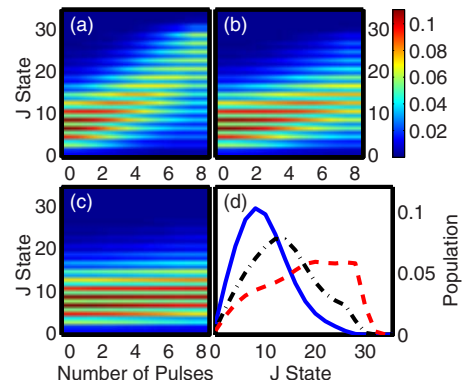


FIG. 4. (Color online) J -state distribution following each pulse for (a) 5.4×10^{13} , (b) 3.6×10^{13} W/cm², (c) 1.7×10^{13} W/cm², and (d) shows the final even- J -state distributions for 5.4×10^{13} W/cm² (dashed), 3.6×10^{13} W/cm² (dash dot), and 1.7×10^{13} W/cm² (solid).

edly nonthermal for the two higher intensities but is very close to thermal for the lowest intensity.

Repeated impulses at the sequence of quantum echoes increases the coherence and redistributes population via impulsive-Raman excitation. For a single pulse, ionization of the sample limits the maximum peak field intensity and therefore limits the maximum kick strength [5]. A pulse train divides the total energy over many pulses and therefore avoids ionization but conserves the subpulse duration. Impulsive Raman processes access the broadest distribution of states when the exciting pulse is shortest. Therefore, dividing energy between multiple pulses while preserving the shortest subpulse duration is an effective way to increase alignment in samples with initially broad rotational distributions. Moreover, this method represents an effective way to achieve coherent distributions centered on very high lying J states, e.g., $\langle J \rangle \sim 25$.

Centrifugal distortion, the primary physical limitation to this technique, causes slightly longer rotational periods for higher rotational levels. It disperses the revival structure of $\rho(t)$ in time causing subsequent pulses to be mistimed with the revivals of the higher lying J states. Therefore, centrifugal distortion limits the number of pulses that can effectively excite a given sample. For instance, a 400 K ensemble of I_2 exhibits significant distortion as early as the half-revival. Even a two-pulse scheme would not work for room temperature I_2 [19] while eight pulses are nearly ideal for N_2 at STP.

We can artificially find a target density matrix that maximizes $\langle \cos^2 \theta \rangle$ given a maximum J state as imposed by centrifugal distortion and laser pulse kick strength for an initial temperature of 300 K [10]. We find that our experimental technique reaches 60% of this artificial maximum value for room temperature nitrogen (see Fig. 5). Figure 5 shows the maximal alignment signal resulting from a single transform-limited pulse in nitrogen at various temperatures, ignoring ionization. Our eight-pulse results come very close to the single-pulse optimal value for a 300 K sample. We note that a single pulse that would create our observed alignment in a 300 K sample would require a peak intensity far above the ionization threshold (vertical line in Fig. 5). We see that our technique achieves alignment very close to what would be expected from single-pulse alignment of a 10 K sample with a peak intensity near the ionization threshold.

The primary finding of this work is that a train of pulses, spaced by the full revival time (τ_{rev}) of the molecules, coinciding with “echoes” of the initial pulse, creates an alignment much greater than an ionization-limited single-pulse. Furthermore, our train of eight pulses exhibits molecular alignment that is nearly identical to a single pulse of the same total pulse energy. We find that eight pulses can allow

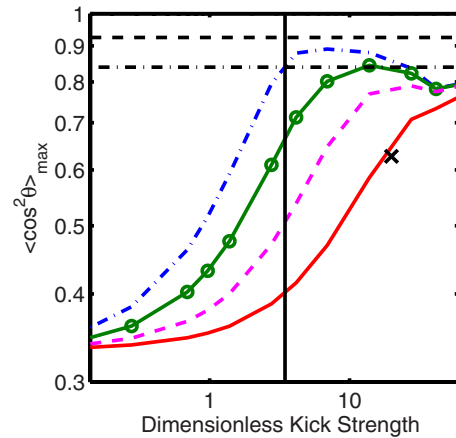


FIG. 5. (Color online) Maximum value of $\langle \cos^2 \theta \rangle$ (including centrifugal distortion), for 50 fs pulses, as a function of dimensionless kick strength $[\Delta\alpha f F(t)^2 dt / (4\hbar)]$ for 0 K (dash-dot), 10 K (circles), 50 K (dashed), and 300 K (solid). Also shown in black, the maximum alignment achievable for a single transform-limited pulse found in Ref. [9] (dashed), the maximum achievable alignment given the maximum J -state from Ref. [10] (dash-dot), and the kick strength of the onset of ionization (5×10^{13} W/cm²) for 50 fs pulses from Ref. [23] (solid). The (x) represents the maximum alignment from our eight-pulse experiment.

the cycle-averaged $\langle \langle \cos^2 \theta \rangle_t \rangle$ to grow larger than the single-pulse transient alignment. Following the eighth pulse, we measure a population alignment of $\langle \langle \cos^2 \theta \rangle_t \rangle \sim 0.43$ and a transient alignment that grows to $\langle \cos^2 \theta \rangle_{\text{max}} \sim 0.63$ in room temperature and atmospheric density nitrogen. Alignment of warm samples has been previously demonstrated but the best reported degree of alignment was only $\langle \cos^2 \theta \rangle \sim 0.36$, vs. a value of 0.33 for an isotropic distribution [16,19].

We have shown that dividing laser energy into pulses spaced by τ_{rev} to coincide with “quantum echoes” of the initial pulse is an effective way to achieve very high degrees of molecular alignment in moderate temperature diatomic gases. Furthermore, multiple pulse excitation of rigid molecules can produce a rotational wave packet whose population is radically different from the initial thermal distribution. In fact, population alignment can grow even larger than the ionization-limited single-pulse transient alignment; this opens the possibility for nontransient field-free aligned molecular ensembles.

The authors would like to acknowledge T. Seideman, S. Ramakrishna, and D. Tannor for their helpful discussions. This work was supported by the United States Department of Energy, Office of Basic Energy Sciences, through the PULSE Institute for Ultrafast Energy Science.

- [1] H. Stapelfeldt and T. Seideman, *Rev. Mod. Phys.* **75**, 543 (2003).
 [2] R. Torres, R. de Nalda, and J. P. Marangos, *Phys. Rev. A* **72**, 023420 (2005).

- [3] F. Rosca-Pruna and M. J. J. Vrakking, *Phys. Rev. Lett.* **87**, 153902 (2001).
 [4] A. Pelzer, S. Ramakrishna, and T. Seideman, *J. Chem. Phys.* **129**, 134301 (2008).

- [5] A. Rouzée, E. Hertz, B. Lavorel, and O. Faucher, *J. Phys. B* **41**, 074002 (2008).
- [6] S. Guérin, A. Rouzée, and E. Hertz, *Phys. Rev. A* **77**, 041404(R) (2008).
- [7] E. Hertz, A. Rouzée, S. Guérin, B. Lavorel, and O. Faucher, *Phys. Rev. A* **75**, 031403(R) (2007).
- [8] I. S. Averbukh and R. Arvieu, *Phys. Rev. Lett.* **87**, 163601 (2001).
- [9] M. Leibscher, I. S. Averbukh, and H. Rabitz, *Phys. Rev. Lett.* **90**, 213001 (2003).
- [10] D. Sugny, A. Keller, O. Atabek, D. Daems, C. M. Dion, S. Guérin, and H. R. Jauslin, *Phys. Rev. A* **72**, 032704 (2005).
- [11] A. G. York and H. M. Milchberg, *Opt. Express* **16**, 10557 (2008).
- [12] M. Leibscher, I. S. Averbukh, and H. Rabitz, *Phys. Rev. A* **69**, 013402 (2004).
- [13] K. F. Lee, I. V. Litvinyuk, P. W. Dooley, M. Spanner, D. M. Villeneuve, and P. B. Corkum, *J. Phys. B* **37**, L43 (2004).
- [14] C. Z. Bisgaard, M. D. Poulsen, E. Peronne, S. S. Viftrup, and H. Stapelfeldt, *Phys. Rev. Lett.* **92**, 173004 (2004).
- [15] C. Z. Bisgaard, S. S. Viftrup, and H. Stapelfeldt, *Phys. Rev. A* **73**, 053410 (2006).
- [16] D. Pinkham and R. R. Jones, *Phys. Rev. A* **72**, 023418 (2005).
- [17] C. W. Siders, J. L. W. Siders, A. J. Taylor, S.-G. Park, and A. M. Weiner, *Appl. Opt.* **37**, 5302 (1998).
- [18] K. Huber, G. Herzberg, J. Gallagher, and I. R. D. Johnson, *NIST Chemistry WebBook* (National Institute of Standards and Technology, Gaithersburg, MD, 2009).
- [19] D. W. Broege, R. N. Coffee, and P. H. Bucksbaum, *Phys. Rev. A* **78**, 035401 (2008).
- [20] B. Lavorel, O. Faucher, M. Morgen, and R. Chaux, *J. Raman Spectrosc.* **31**, 77 (2000).
- [21] N. G. Theofanous, *J. Opt. Soc. Am. A* **4**, 2191 (1987).
- [22] J. Ortigoso, M. Rodriguez, M. Gupta, and B. Friedrich, *J. Chem. Phys.* **110**, 3870 (1999).
- [23] C. Guo, M. Li, J. P. Nibarger, and G. N. Gibson, *Phys. Rev. A* **58**, R4271 (1998).